Available online at www.sciencedirect.com

SciVerse ScienceDirect

Ceramics International 39 (2013) S41–S45

CERAMICS INTERNATIONAL

www.elsevier.com/locate/ceramint

Preparation and dielectric properties of $(Sr_{1-x}Ca_x)Fe_{0.5}Nb_{0.5}O_3$; ($x=0.0$, 0.1, 0.2) ceramics

Thanatep Phatungthane, Gobwute Rujijanagul*

Department of Physics and Materials Science, Faculty of Sciences, Chiangmai University, Huaykaw Road, Chiangmai 50200, Thailand

Available online 23 October 2012

Abstract

In the present work, strontium calcium iron niobate ($(Sr_{1-x}Ca_x)Fe_{0.5}Nb_{0.5}O_3$; SCFN) ($x=0$, 0.1, and 0.2) powders were synthesized for the first time using a molten salt technique. The pure phase perovskite obtained at a relative low calcination temperature of 800 °C was characterized using the X-ray diffraction technique (XRD). SCFN ceramics were fabricated and their properties were investigated. The XRD data of the SCFN ceramics was consistent with an orthorhombic symmetry. However, the solubility of Ca in the SCFN ceramics had an upper limit at $x=0.1$. All ceramics showed a large dielectric constants. The Ca doping inhibited grain growth, but produced an improvement in dielectric–temperature stability. Furthermore, the doping reduced loss tangent, especially for the $x=0.1$ sample. These results suggest that the SCFN ceramics prepared from molten salt synthesis exhibit a good dielectric performances, compared to many high dielectric materials that have been prepared using the conventional method.

Keywords: D. Perovskite; High dielectric; Relaxor

1. Introduction

Ceramics with high dielectric constants and giant dielectric constants with a perovskite structure of AB'B''O_3 have been extensively developed due to their potentials for capacitor applications [1,2]. The complex structure $A(Fe_{0.5}B_{0.5})O_3$ with $A=$ Sr, Ca, Pb; $B=$ Nb, Ta, and Sb are all perovskite type ceramics which exhibit giant dielectric behavior [1,2]. For example, the ceramic $Ba(Fe_{0.5}Nb_{0.5})O_3$ (BFN) exhibits a high value for the dielectric constant ($\varepsilon_r \sim 10^3$–10^4) over a wide range of temperatures [2,3]. BFN was first synthesized via a solid-state reaction by Saha and Sinha in 2002 [4,5]. Since then many authors have focused on the properties of these BFNs. Works from Yokosuka [6], Tezuka et al. [7], Raevski et al. [3], Saha and Sinha [4,5] have shown that the BFN-based ceramics have a relaxor behavior. Furthermore, Shanming et al. demonstrated that the value of ε_r of the BFN ceramics depend on processing parameter [8].

$Sr(Fe_{0.5}Nb_{0.5})O_3$ (SFN) is another interesting dielectric material due to its high dielectric constant. The dielectric properties of the SFN ceramics were first reported by Raevski et al. [3]. These materials have high dielectric constants on the order of 10^3–10^4 over a wide frequency and a broad temperature range [3]. The high dielectric behavior has been interpreted in terms of the Maxwell–Wagner mechanism [3]. SFN ceramics also exhibit a dielectric relaxation behavior, similar to other giant dielectric materials such as $Ba(Fe_{0.5}Nb_{0.5})O_3$ and $Ba(Fe_{0.9}Al_{0.1})$-$Ta_{0.5}O_3$ [3–7,9]. The magnetic properties of the SFN at low temperatures (lower than 100 K) were reported by Tezuka et al. [7] The ferroelectric properties of SFNs could be improved by forming a solid–solution with $PbTiO_3$ combined with MnO_2 or Li_2CO_3 doping [10]. However, the effects of doping on the properties of these SFN ceramics have not been widely investigated. Furthermore, it should be noted that most $A(Fe_{0.5}B_{0.5})O_3$ ceramics were synthesized using a solid-state reaction method (the conventional method). This method often requires a high calcination temperature which can cause particle coarsening and aggregation of the powders. Therefore, other routes including the sol–gel process, hydrothermal synthesis and molten salt synthesis have been employed produce fine powders [11–13]. Among these methods, molten salt

*Corresponding author. Tel.: +6653943376; fax: +66533575112.
E-mail address: rujijanagul@yahoo.com (G. Rujijanagul).

0272-8842/$ - see front matter © 2012 Elsevier Ltd and Techna Group S.r.l. All rights reserved.
http://dx.doi.org/10.1016/j.ceramint.2012.10.032

synthesis is a simple and practical technique with low costs for powder preparation. In the present work, we report the effects of Ca doping on the properties SFN ceramics. The SFN powder and Ca doped SFNs were synthesized via the molten salt synthesize for the first time.

2. Experimental

Strontium calcium iron niobate $(Sr_{1-x}Ca_x)Fe_{0.5}Nb_{0.5}O_3$; ($x=0.0$, 0.1, 0.2) samples were synthesized using the molten salt technique from high purity raw powders of $SrCO_3$ (98.0%, Aldrich), Fe_2O_3 (99.0%, Aldrich), Nb_2O_5 (99.9%, Aldrich), and $CaCO_3$ (98.5%, Riedel-de Haël]n). The raw metal oxide powders were weighed based on the stoichiometric formula of $(Sr_{1-x}Ca_x)Fe_{0.5}Nb_{0.5}O_3$, then ball milled in alcohol and zirconia milling media for 24 h. The mixture was dried at 110 °C for 12 h. An equal molar ratio of salt mixtures, NaCl (99.5%, Fluka) and KCl (99.5%, Riedel-de Haen) were mixed by hand-grinding for 20 min. The mixed precursors and mixed salts were weighed into a 1:1 ratio. After hand-grinding for 30 min, the obtained powders were calcined at 800 °C for 3 h with a heating rate of 100 °C/h and cooling rate of 300 °C/h. The products were washed with hot deionized water for several times until no trace of anion was detected by $AgNO_3$ aqueous solution. The obtained powders were then added with 3% polyvinyl alcohol (PVA) and pressed into disc compact shapes with a diameter of 1.00 cm. These green compacts were then sintered at temperatures ranging from 1300 °C to 1450 °C for 3 h with the same conditions of that of the calcination rate. The phase formation was identified using the X-ray diffraction technique (XRD). The microstructures were then examined using a scanning electron microscope (SEM). To investigate the electrical properties, the sintered ceramic pellets were painted with silver paste on both sides and fried at 600 °C for 15 min. The electrical characteristics were then evaluated using an LCR meter.

3. Results and discussion

In the present work, the mixed raw powders were calcined over a temperature range 600–900 °C. Selected XRD patterns of the obtained powders are illustrated in the inset of Fig. 1. The XRD results indicate that the $x=0.0-0.1$ samples exhibited a pure perovskites structure at a calcination temperature of 800 °C. Generally, the pure phase of SFN can be synthesized at the calcination temperature of 1200 °C by using the solid-state reaction method [14,15]. Thus, the presence of pure phase SFN at 800 °C in the present work, suggests that the molten salt synthesization method can reduce the calcination temperature by 400 °C.

Fig. 1 also shows the X-ray patterns of the studied ceramics. These XRD results show that the diffraction peaks of the ceramics correspond to an orthorhombic perovskite phase. This result agrees with the work done by

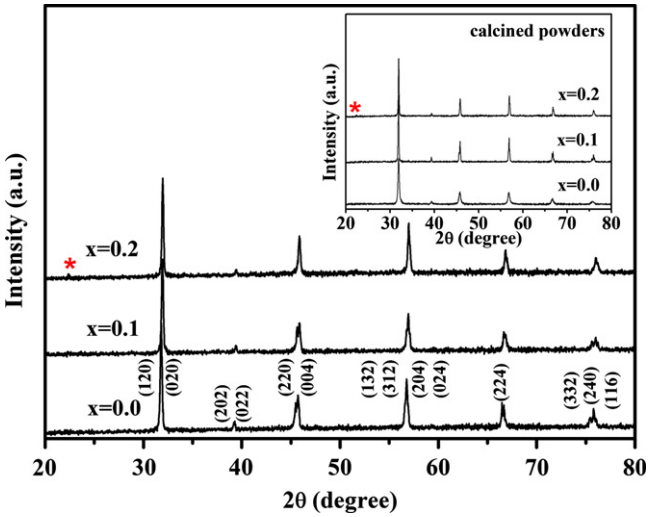

Fig. 1. XRD patterns of $Sr_{1-x}Ca_xFe_{0.5}Nb_{0.5}O_3$ (SCFN) powders and ceramics.

Liu et al. [15]. The appearance of three main peaks of (332), (240), and (116) with reflections at $2\theta \sim 75–77°$, confirms the presence of the orthorhombic phase for the studied samples. However, the three main peaks merged into an ambiguous peak at the higher Ca concentration ($x=0.2$). Furthermore, a pure perovskite phase was observed for $x \leq 0.1$ samples. Extra impurity peaks were observed and indexed (by $*$), as seen in Fig. 1. This second phase was identified as Ca_2FeNbO_6 according to the JCPDS file no. 01-089-1442. The appearance of the second phase for the $x=0.2$ sample, indicates that the solubility of Ca in SFN had a low limit. The unit-cell volume of the samples calculated based on orthorhombic symmetry was found to decrease from 251.22 (Å^3) for the $x=0.0$ sample to 249.57 (Å^3) for the $x=0.2$ sample. This decrease in unit-cell volume with increasing Ca content indicates an introduction of Ca ions in the SFN lattice. In general, the solubility of a dopant in a lattice depends not only on the charge but also on the radius of the dopant. The charge of Ca^{2+} ion is the same as that of Sr^{2+} and the radius of the Ca^{2+} ion (0.134 nm) is close to that of the Sr^{2+} ions (0.144 nm). Therefore, it is possible that partial Ca^{2+} ions substituted Sr^{2+} ions in the lattice as a result in the decrease of unit-cell volume.

The SEM micrographs of the selected ceramic surfaces are illustrated in Fig. 2. The micro structural analysis revealed that Ca doping result in a change in grain size. Average values of grain size, as calculated by the linear intercept method, decreased from ~11.1 μm for the pure SFN ceramic to ~6.4 μm for the $x=0.2$ ceramic. This result indicates that the additive inhibits grain growth. This may be due to the low solubility limit of Ca in the SFN lattice, resulting in the formation of the secondary phase which may form at the grain boundaries and prevent grain boundary movement during the sintering process [16].

The dielectric constant and loss tangent as a function of frequency at room temperatures is shown in Fig. 3.

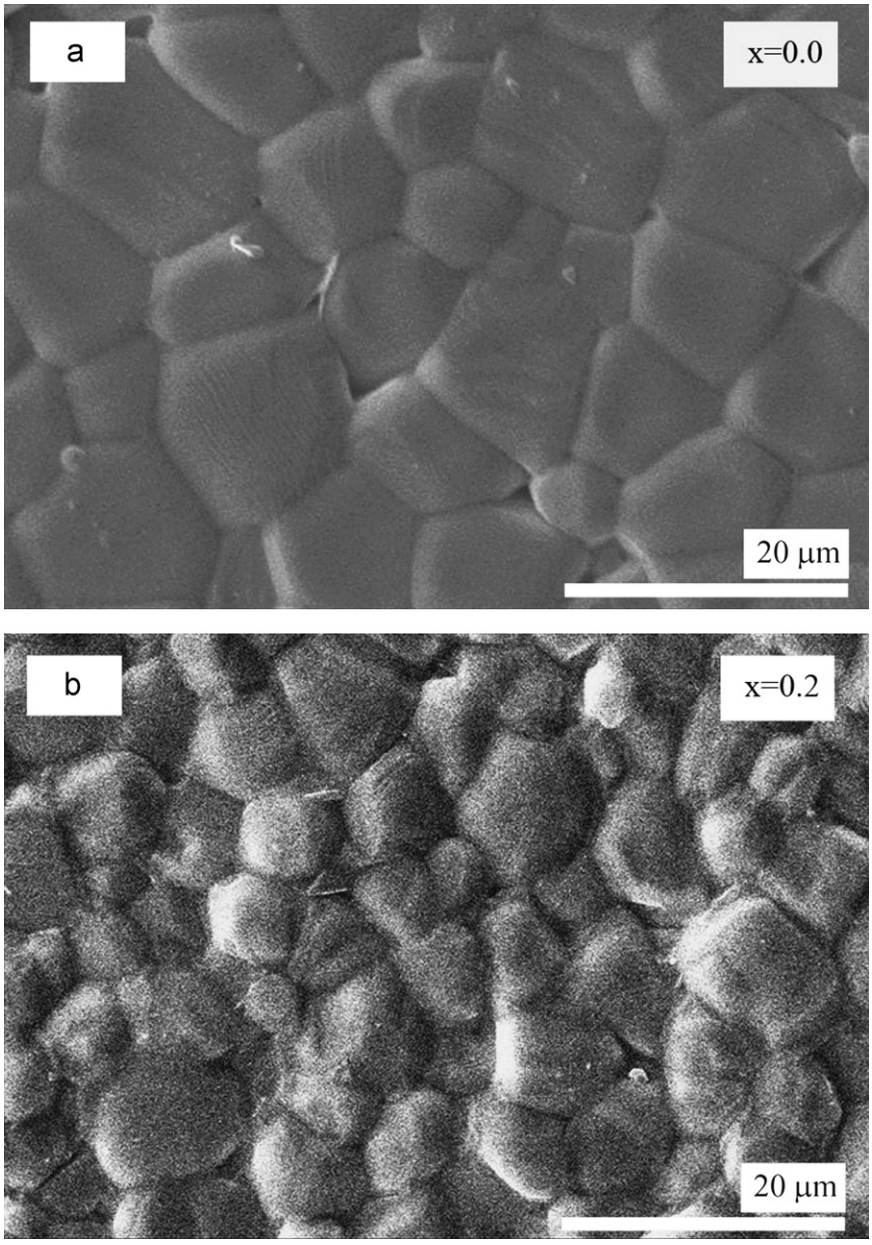

Fig. 2. SEM micrographs of (a) $x=0.0$ and (b) $x=0.2$ of SCFN ceramics.

For pure SFN ceramics, the dielectric constant at 1 kHz was ~11,200 which is high compared to many high dielectric ceramics that were fabricated using the conventional technique [2,15]. Further, all presented samples exhibited high dielectric constants especially at lower frequencies (the dielectric constant versus frequency in log scale is shown in the inset of Fig. 3). However, the dielectric constant of all samples decreased with increasing frequencies. A similar behavior was found by Intatha et al. who investigated the properties of BFN ceramics [17]. The loss tangent values as a function of frequency with different Ca concentrations are also shown in Fig. 3. The general trend of the loss tangent value over the frequency range for the doped samples is similar to that observed in some giant dielectric material such as $CaCu_3Ti_4O_{12}$ (CCTO) [18,19] where the loss tangent behavior of CCTO was related to microstructure characteristics [19]. However, all samples showed a peak of the loss tangent for frequencies $> \sim 2.5 \times 10^5$ Hz.

Fig. 4 shows plots of the dielectric constant and loss tangent (at 1 kHz) as a function of temperature at various Ca concentrations. Each sample showed an increase in dielectric constant with temperature. This behavior is similar to that reported in previous work on SFN and BFN ceramics [15,17]. The dielectric constant in the temperature range 27–95 °C increases with increasing Ca concentrations. However, the dielectric constants of the doped samples at temperatures > 95 °C were relatively low

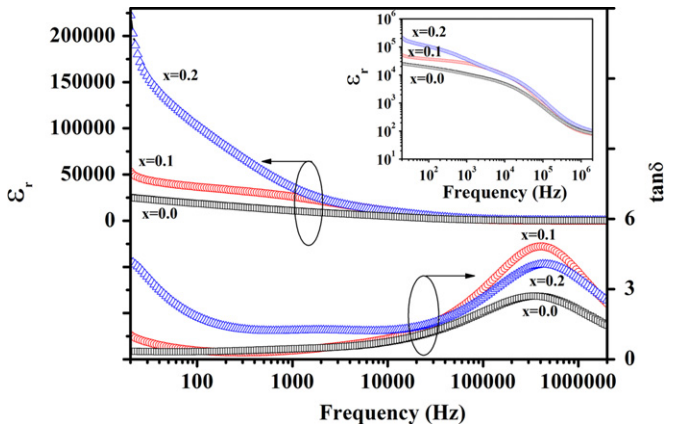

Fig. 3. Frequency dependence of ε_r and tanδ of SCFN ceramics for room temperature.

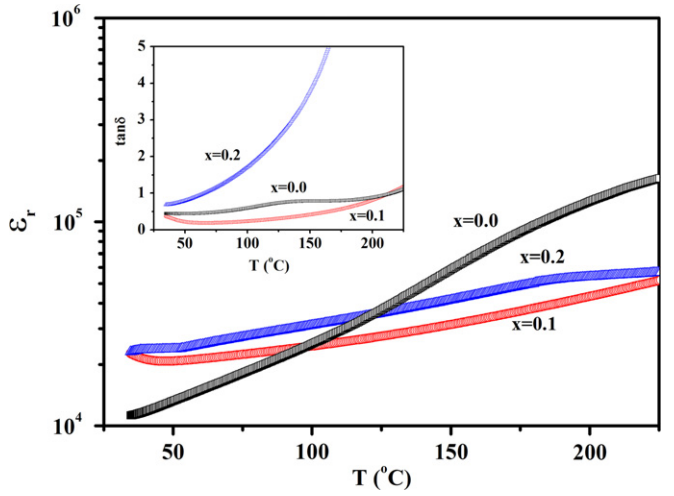

Fig. 4. Temperature dependence of ε_r and tanδ of SCFN ceramics for 1 kHz.

compared to the undoped samples. This result indicates that Ca doping produced a higher degree of temperature dielectric stability. It should be noted that the generated samples exhibited a high loss tangent. This may be due to oxygen non-stoichiometry and/ or cation non-stoichiometry in the samples [20]. However, the Ca doping reduced the loss tangent value for the $x=0.1$ sample (inset of Fig. 4). The change in dielectric behavior is unclear but could be linked to the microstructure since there were changes in microstructure after doping. Further, heterogeneous composition and the presence of a second phase in the samples after doping are considered to be other reasons for these behaviors. However, the dielectric constant values observed in the present work are still considered to be high for giant dielectric ceramics.

4. Conclusions

The molten salt technique was employed to synthesize the SCFN powders. This technique was able to reduce the calcinations temperature to a very low temperature compared to the conventional method. The pure phase powders were then used to form SCFN ceramics. All ceramics showed high dielectric constants while the doped ceramics also exhibited the better dielectric–temperature stability and a lower loss tangent (compared to SFN ceramic). Based on the advantage of molten salts synthesize, it is interesting to apply this technique for preparation of other electro ceramic materials for future work.

Acknowledgments

This work was supported by The Royal Golden Jubilee Ph.D. Program, Faculty of Science and Graduate School Chiang Mai University and National Research University (NRU), Office of the Higher Education Commission (OCHE) Thailand.

References

[1] I.M. Reaney, J. Petzelt, V.V. Voitsekhovskii, F. Chu, N. Setter, B-site order in infrared reflectivity in AB'BO_3 complex perovskite ceramics, Journal of Applied Physics 76 (1994) 2086–2092.
[2] K. Prasad, K.P. Chandra, S. Bhagat, S.N. Choudhary, A.R. Kulkarni, Structural and electrical properties of lead-free perovskite $Ba(Al_{1/2}Nb_{1/2})O_3$, Journal of the American Ceramic Society 93 (2010) 190–196.
[3] I.P. Raevski, S.A. Prosandeev, A.S. Bogatin, M.A. Malitskaya, L. Jastrabik, High dielectric permittivity in $AFe_{1/2}B_{1/2}O_3$ nonferroelectric perovskite ceramics (A=Ba, Sr, Ca; B=Nb, Ta, Sb), Journal of Applied Physics 93 (2003) 4130–4136.
[4] S. Saha, T.P. Sinha, Structural and dielectric studies of $BaFe_{0.5}Nb_{0.5}O_3$, Journal of Physics: Condensed Matter 14 (2002) 249–258.
[5] S. Saha, T.P. Sinha, Low-temperature scaling behavior of $BaFe_{0.5}Nb_{0.5}O_3$, Physical Review B 65 (2002) 134103.
[6] M. Yokosuka, Dielectric dispersion of the complex perovskite oxide $Ba(Fe_{1/2}Nb_{1/2})O_3$ at low frequencies, Japanese Journal of Applied Physics 34 (1995) 5338–5340.
[7] K. Tezuka, K. Henmi, Y. Hinatsu, N.M. Masaki, Magnetic susceptibilities and Mossbauer spectra of perovskites A_2FeNbO_6 (A=Sr, Ba), Journal of Solid State Chemistry 154 (2000) 591–597.
[8] S. Ke, H. Huang, H. Fan, H.L.W. Chan, L.M. Zhou, Colossal dielectric response in barium iron niobate ceramics obtained by different precursors, Ceramics International 34 (2008) 1059–1062.
[9] Z. Wang, X.M. Chen, X.Q. Liu, $Ba[(Fe_{0.9}Al_{0.1})_{0.5}Ta_{0.5}]O_3$ ceramics with extended giant dielectric constant step and reduced dielectric loss, Journal of Applied Physics 105 (2009) 034114.
[10] B. Fang, Z. Cheng, R. Sun, C. Ding, Preparation and electrical properties of $(1-x)Sr(Fe_{1/2}Nb_{1/2})O_{3-x}PbTiO_3$ ferroelectric ceramics, Journal of Alloys and Compounds 471 (2009) 539–543.
[11] X. Yana, W. Ren, X. Wu, P. Shi, X. Yao, Lead-free (K, Na)NbO_3 ferroelectric thin films: preparation, structure and electrical properties, Journal of Alloys and Compounds 508 (2010) 129–132.
[12] Y. Zhou, M. Guo, C. Zhang, M. Zhang, Hydrothermal synthesis and piezoelectric property of Ta-doping $K_{0.5}Na_{0.5}NbO_3$ lead-free piezoelectric ceramic, Ceramics International 35 (2009) 3253–3258.
[13] F. Bortolani, R.A. Dorey, Molten salt synthesis of PZT powder for direct write inks, Journal of the European Ceramic Society 30 (2010) 2073–2079.
[14] S. Saha, T.P. Sinha, Dielectric relaxation of $SrFe_{1/2}Nb_{1/2}O_3$, Journal of Applied Physics 99 (2006) 014109.
[15] Y.Y. Liu, X.M. Chen, X.Q. Liu, L. Li, Giant dielectric response and relaxor behaviors induced by charge and defect ordering in $Sr(Fe_{1/2}Nb_{1/2})O_3$ ceramics, Applied Physics Letters 90 (2007) 192905.

[16] S.H. Lee, C.B. Yoon, S.B. Seo, H.E. Kim, Effect of lanthanum on the piezoelectric properties of lead zirconate titanate–lead zinc niobate ceramics, Journal of Materials Research 18 (2003) 1765–1770.
[17] U. Intatha, S. Eitssayeam, J. Wang, T. Tunkasiri, Impedance study of giant dielectric permittivity in $BaFe_{0.5}Nb_{0.5}O_3$ perovskite ceramic, Current Applied Physics 10 (2010) 21–25.
[18] L. Ni, X.M. Chen, X.Q. Liu, R.Z. Hou, Microstructure-dependent giant dielectric response in $CaCu_3Ti_4O_{12}$ ceramics, Solid State Communications 139 (2006) 45–50.
[19] L. Feng, X. Tang, Y. Yan, X. Chen, Z. Jiao, G. Cao, Decrease of dielectric loss in $CaCu_3Ti_4O_{12}$ ceramics by La doping, Physica Status Solidi (A) 203 (2006) 22–24.
[20] T.B. Adams, D.C. Sinclair, A.R. West, Decomposition reactions in $CaCu_3Ti_4O_{12}$ ceramics, Journal of the American Ceramic Society 89 (2006) 2833–2838.